Visible range colossal magnetorefractive effect in $(La_{1-y}Pr_y)_{2/3}Ca_{1/3}MnO_3$ films

2014 New J. Phys. 16 063034

(http://iopscience.iop.org/1367-2630/16/6/063034)

New Journal of Physics
The open access journal at the forefront of physics
Deutsche Physikalische Gesellschaft DPG | IOP Institute of Physics

Visible range colossal magnetorefractive effect in $(La_{1-y}Pr_y)_{2/3}Ca_{1/3}MnO_3$ films

M Jungbauer, S Hühn, J-O Krisponeit and V Moshnyaga
I. Physikalisches Institut, Georg-August-Universität Göttingen, Friedrich-Hund-Platz 1, 37077 Göttingen, Germany
E-mail: vmosnea@gwdg.de

Received 26 February 2014, revised 6 May 2014
Accepted for publication 27 May 2014
Published 17 June 2014
New Journal of Physics **16** (2014) 063034
doi:10.1088/1367-2630/16/6/063034

Abstract
We report a colossal magnetorefractive effect (MRE) in epitaxial thin films of a classical colossal magnetoresistance (CMR) manganite, $(La_{1-y}Pr_y)_{2/3}Ca_{1/3}MnO_3$ ($y = 0.375$ and 0.7). Close to the ferromagnetic (FM) phase transition a moderate applied magnetic field, $H \sim 10$ kOe, results in a reduction of the optical reflectance by ~18% for the photon energy $E \sim 2.7$ eV. The MRE spectral behavior with three pronounced maxima at $E = 1.6$, 2.7 and 4.0 eV points out an inter-site nature of the involved optical transitions. The results are discussed within a phase separation scenario with coexisting FM metallic nanodomains antiferromagnetically coupled by correlated polarons. The probability of MRE optical transitions is maximal for antiparallel alignment of Mn^{3+}/Mn^{4+}-spins realized for the coercive field, $H_c \sim 200$–800 Oe, and is suppressed by stronger fields, which favor FM metallic behavior. As a result, both the optical reflectivity and the electrical resistance decrease, yielding a close similarity between the CMR and MRE behavior.

Keywords: manganite films, colossal magnetoresistance, optical reflectivity

1. Introduction

Colossal magnetoresistant (CMR) [1] perovskite manganites remain in the focus of modern correlation physics due to a number of phase transitions, like metal–insulator (MI),

ferromagnetic–paramagnetic (FM–PM) as well as structural phase transitions. It is commonly believed that strong electronic and spin correlations together with the electron–phonon coupling are responsible for a rich phase diagram containing different electronic, magnetic and structural phases [2]. In addition, these transitions can be strongly influenced by external (hydrostatic pressure, magnetic and electric fields, electromagnetic radiation) and internal (chemical pressure, doping) control parameters, leading to drastic changes in the magnetotransport. To explain the huge reduction of the electrical resistance in an applied field of a few tesla, e.g. $\mathrm{CMR} = (R(0)–R(B))/R(B) = 10^5–10^8$, an electronic phase separation (EPS) scenario was proposed [2, 3]. Close to the Curie temperature, T_C, the coexisting FM metallic and charge-ordered insulating (COI) phases may have a similar free energy, so that a relatively low applied magnetic field, favoring the FM-phase, may cause the MI transition due to the formation of percolating paths of the metallic phase through the sample [2, 4–6]. Very recently [7] we have shown that EPS in thin films of a classical CMR manganite, i.e. $(La_{1-y}Pr_y)_{2/3}Ca_{1/3}MnO_3$ (LPCMO) with Pr-doping, $y \sim 0.4$, develops at the nanometer scale, where FM nanodomains are intrinsically antiferromagnetic (AFM) exchange coupled by correlated Jahn–Teller (JT) polarons. The latter, dubbed in the literature as 'polaronic phase' or 'correlated polarons', have been experimentally detected by neutron scattering [8, 9] and x-ray diffraction [10] in the form of short-range-ordered lattice superstructures of CE-type with correlation length 1–2 nm. By means of isovalent substitution of a large La^{3+} cation by a smaller Pr^{3+} in the optimally hole-doped $La_{2/3}Ca_{1/3}MnO_3$ (LCMO) an increase of electron–phonon interaction favors the tendency to phase competition [11]. The FM metallic ground state for $y = 0$ progressively transforms with increasing 'y' into a mixture of FM metallic and AFM COI phases [3, 12].

An increase of the optical conductivity in an applied magnetic field, originally named the magnetorefractive effect (MRE), was first observed in the giant-magnetoresistive (GMR) structures, where MRE manifests itself as a high-frequency continuation of GMR [13]. For perovskite manganites, e.g. LCMO, an increase of the optical conductivity in an applied magnetic field for the infrared (IR) region of spectrum, $E < 1.0$ eV, was predicted theoretically [14, 15]. Experimentally, a magnetoconductivity effect, $\Delta\sigma(\mathrm{B})/\sigma(0) \sim -50\%$ ($B = 16$ T), was observed and called 'optical CMR' [16]. In contrast, the optical conductivity in LCMO for photons in the visible range, $E > 1–1.5$ eV, decreases in an applied magnetic field as well as upon decreasing temperature, $T < T_C$. The reason is a spectral weight transfer [17] from the exchange-split inter-band optical transitions at high energies to intra-band transitions at low energies (Drude-like conductivity). Such behavior is common for strongly correlated electronic oxide systems with MI transition even in the absence of magnetic transition [18]. The transferred spectral weight in a double exchange FM manganite, i.e. $La_{0.7}Sr_{0.3}MnO_3$ (LSMO), is proportional to the square of the magnetization [17]. In CMR materials, like LCMO with relatively large electron–phonon coupling, this correlation is not so straightforward—one has to consider the corrections to the one-electronic bandwidth due to the JT effect [19]. Recently, a small visible light MRE (reflectivity decreases by ~1–2%) was detected in LCMO thin films at $T \sim T_C$ and explained as JT resonances [20], which are related to the same phenomenon of spectral weight transfer. For phase separated CMR manganites with large electron–phonon coupling, e.g. LPCMO, the IR optical conductivity looks more complicated and provides evidences for the coexistence of different electronic phases [12]. However, the relation between ac and dc magnetic-field-induced effects, i.e. MRE and CMR, is not sufficiently understood.

Here we report a colossal MRE for visible light in epitaxial and strain-free LPCMO/MgO (100) films. A correlation between dc resistance (CMR) and ac (optical) conductivity (MRE)

with hysteretic field and temperature dependencies close to phase transition was demonstrated. This indicates that colossal MRE behavior is caused by the existence of a short-range ordered polaronic AFM COI phase, which provides the optically active inter-site (inter-band) transitions between Mn^{3+}/Mn^{4} ions with antiparallel aligned spins.

2. Samples and experimental techniques

For the optical study LPCMO films with Pr-doping $y = 0.375$ and 0.7 and thicknesses $d \simeq 70$ nm were chosen. The films were prepared by a metalorganic aerosol deposition technique [21, 22]. A heteroepitaxial growth on MgO(100) substrates and a strain-free state of LPCMO was evidenced by transmission electron microscopy and x-ray diffraction [7]. The films were characterized by magnetization and four-point resistance, measured by means of MPMS (SQUID) and PPMS from 'Quantum design', respectively. The optical reflectivity at normal incidence was monitored for photon energies, $E = 1.5$–4.1 eV, and in-plane magnetic fields, $H = 0$–10 kOe, created by an electromagnet. Simultaneously with the reflectivity, measured within the diameter of the light spot, $\varnothing \sim 3$ mm, the dc resistance from the same illuminated region was recorded by 4-point technique. The relative change of the reflectivity, Ref, in applied field is a measure of MRE, therefore we define:

$$\mathrm{MRE}\,(T, H, E) = 100\% \times [\mathrm{Ref}\,(0) - \mathrm{Ref}\,(H)\,]/\mathrm{Ref}\,(H) \tag{1}$$

to quantify the observed changes. In the following we use the term MRE to refer to changes in the reflectivity induced by applied magnetic field. To quantify the changes of the resistance, R, we define:

$$\mathrm{CMR}\,(T, H) = 100\% \times [R\,(0) - R\,(H)\,]/R\,(H). \tag{2}$$

These quantities were measured for temperatures, $T = 10$–300 K, and magnetic fields, $H = 0$–10 kOe, as well as in the spectral range, $E = 1.5$–4.1 eV (MRE).

3. Results

Temperature dependences of the resistance, $R(T)$, shown in figure 1(a), reveal sharp MI transitions at temperatures $T_{\mathrm{MI}} \sim 190$ and 100 K for films with $y = 0.375$ and 0.7, respectively. The sharpness of MI transitions is characterized by large values of the dimensionless parameter, $\alpha_R = (T/R)(\mathrm{d}R/\mathrm{d}T) = 80$ and 250 for films with $y = 0.375$ and 0.7, respectively. The magnetic and MI transitions are coupled, $T_{\mathrm{MI}} \sim T_{\mathrm{C}}$ (see figure 1(b)), indicating an intrinsic nature of the first order phase transition in the LPCMO films under study and the minor role of extrinsic effects (chemical disorder and/or grain boundaries). A huge cooling-warming hysteresis in $R(T)$ and $M(T)$ curves, $\Delta T = 30$ K, in the heavily doped sample ($y = 0.7$) is in line with the enhancement of the phase separation tendency by increasing of Pr-doping. In contrast, a small hysteresis, $\Delta T < 1$ K, was observed in $y = 0.375$ film.

The characteristic feature in LPCMO films was the reduction of optical reflectance while cooling down across T_{C} into the FM state. As shown in figure 1(b), the reflectivity of the $y = 0.375$ sample reduces by about 40% for $T \ll T_{\mathrm{C}}$ as compared to that in the PM state. Qualitatively the change of reflectance resembles $M(T)$, signaling the magnetic origin of optical changes. Note that $M(T)$ was measured in applied field, $H = 100$ Oe, whereas the reflectance in figure 1(b) was taken in an ambient field. Magnetic-field-induced changes of the reflectance, i.e.

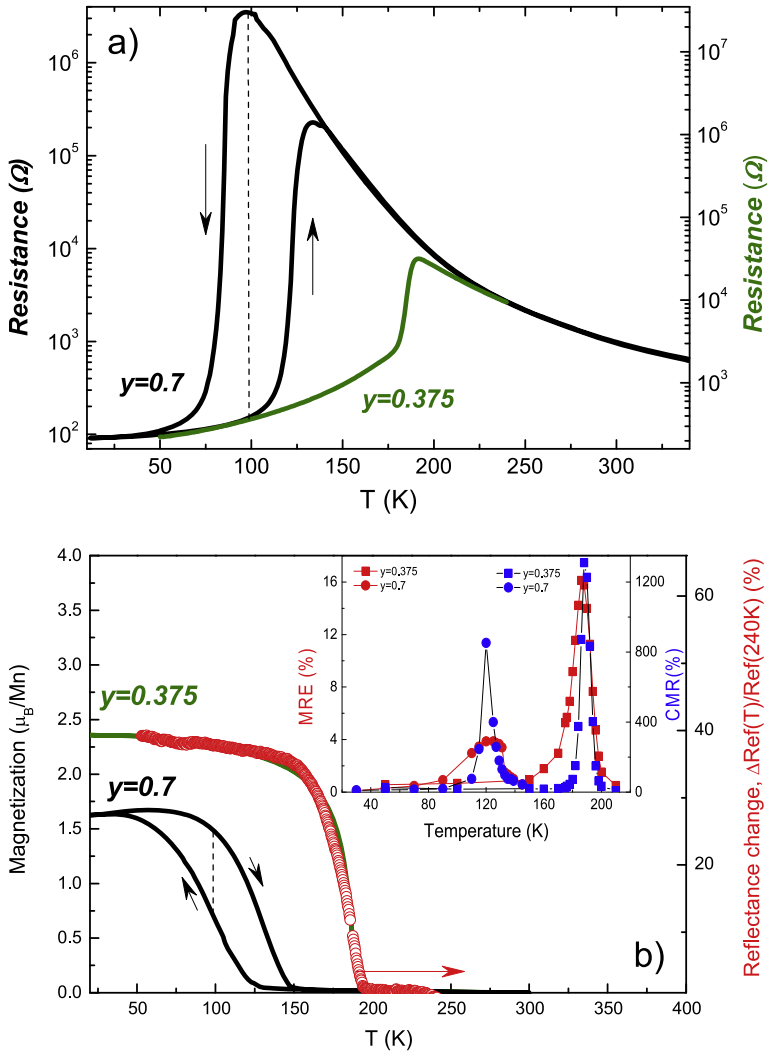

Figure 1. Temperature dependences of electrical resistance in ambient magnetic field (a) and magnetization (b) in the field-cooling (FC) mode ($H = 100$ Oe) for LPCMO films with Pr-doping, $y = 0.375$ (green, right scale in (a)) and $y = 0.7$ (black, left scale in (a)). The reflectance (red curve, $\lambda = 827$ nm) for sample $y = 0.375$ is shown in (b). The inset in (b) demonstrates a similarity between the temperature behavior of CMR and MRE: both quantities are maximal close to T_C. For the $y = 0.7$ sample a small MRE is due to the FC state.

MRE, are found to be maximal at the phase transition (see inset to figure 1(b)) and are similar to the temperature behavior of CMR. In addition, the $y = 0.375$ sample reveals MRE = 17% and CMR = 1300%, which are significantly larger than those measured for the $y = 0.7$ sample, i.e. MRE = 4% and CMR = 900% ($H = 10$ kOe), obtained in the field-cooling (FC) mode.

In figure 2 one can see magnetic field dependences of the resistance (CMR) and reflectivity (MRE for $\lambda = 827$ nm) for a LPCMO-film with $y = 0.375$. For $T < T_C$ and $T > T_C$ the CMR(H) and MRE(H) scale quite well with each other. Very close to T_C (figure 2(b)) and for low fields, -5 kOe $< H < 5$ kOe, both MRE and CMR show a similar hysteretic behavior. For very low ($T < 50$ K) and for high temperatures ($T \gg T_C$) no magnetic-field-induced changes in the optical

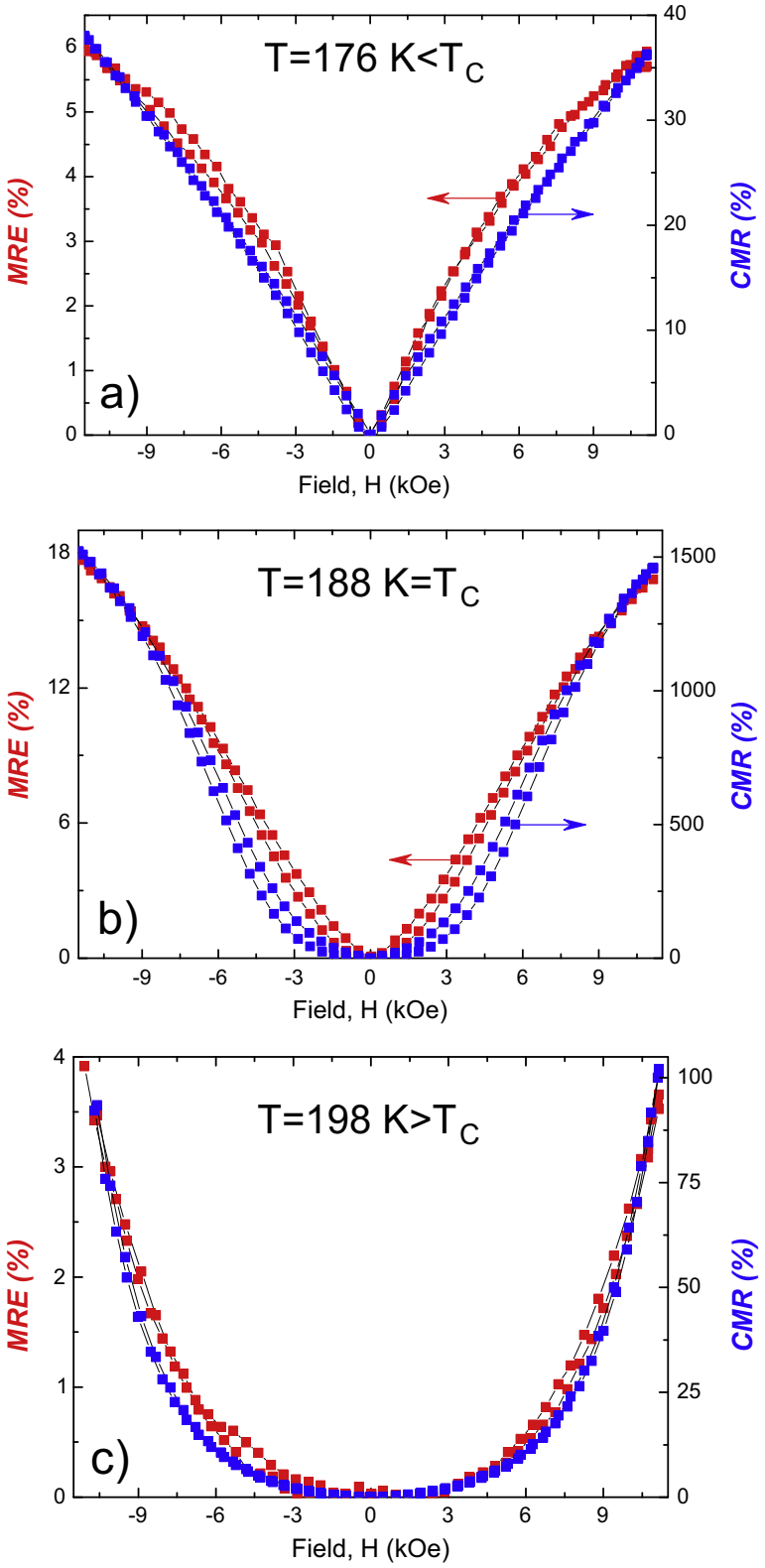

Figure 2. Magnetic field dependences of the normalized electrical resistance (blue symbols) and optical reflectance ($\lambda = 827$ nm, red symbols) in LPCMO film with Pr-doping $y = 0.375$, measured for: (a) $T < T_C$; (b) $T = T_C$; (c) $T > T_C$.

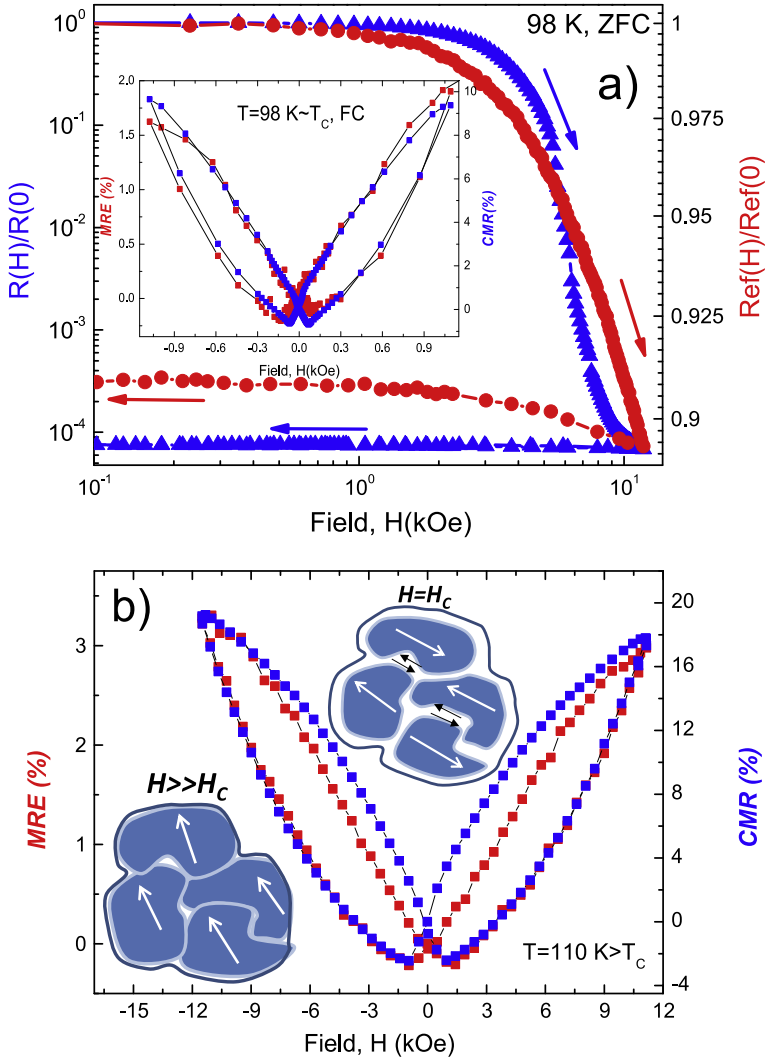

Figure 3. Hysteretic field dependences of CMR (blue symbols) and MRE ($\lambda = 827$ nm, red symbols) for LPCMO with $y = 0.7$: (a) after zero-field cooling down to 98 K, at which the resistance is maximal. The inset shows the CMR and MRE loops in FC; (b) for $T = 110$ K within the phase separated state in the vicinity of T_C. The insets show AFM coupled FM magnetic nanodomains at $H = H_C$ (middle) and parallel aligned domains at $H \sim 10\,\text{kOe} \gg H_c$ in the absence of correlated polarons.

reflectivity and in the resistance were detected (not shown). For the heavily Pr-doped sample ($y = 0.7$), a huge temperature hysteresis, $\Delta T \sim 30$ K, in $M(T)$ and $R(T)$ in the vicinity of phase transition (see figure 1), correlates well with the pronounced field hysteresis in MRE and CMR, shown in figure 3. A FC in $H = 10$ kOe pushes the system into a low-resistance state, which can also be obtained by warming up in zero field. The strong hysteretic changes in the reflectivity for the $y = 0.7$ sample were obtained under zero-field-cooling (ZFC) down to $T = 98$ K, at which the resistance is maximal. By applying a magnetic field both resistance and reflectivity drop as shown in figure 3(a). During the following reduction of magnetic field the resistance remains almost constant, whereas the reflectivity increases slightly. Remarkably, the CMR(H) and MRE(H) dependences in the FC mode (inset of figure 3(a), figure 3(b)) reveal a characteristic

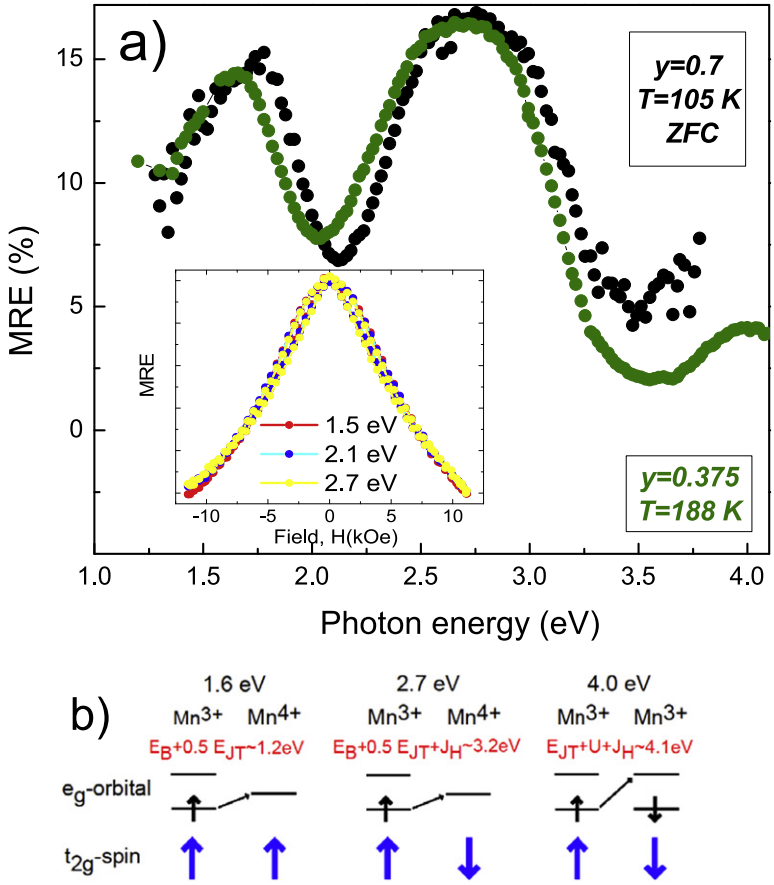

Figure 4. (a) MRE spectra for LPCMO films ($y = 0.375$ and 0.7) taken close to T_C with $H = 10$ kOe. The inset shows the field dependence of the normalized reflectivity in $y = 0.375$ for $T \sim T_C$ for different photon energies; (b) e_g–e_g intersite transitions between neighboring Mn ions which might be responsible for spectral dependence of MRE. The energies for the assumed transitions are estimated with the correlation energies, taken from [2]: Hund's energy $J_H \approx 2$ eV, the Jahn–Teller splitting $E_{JT} \approx 0.8$ eV, the Coulomb repulsion $U \approx 1.7$ eV. The breathing mode distortion energy, $E_B \approx 0.8$ eV, is taken from [28, 30].

'butterfly-like' form with two maxima at the coercive field H_c. This behavior is characteristic for both samples ($y = 0.375$ and 0.7), but it is especially pronounced for the heavily doped sample in the hysteretic region close to the phase transition.

To shed light on the microscopic origin of the colossal MRE the spectral dependence of the effect was measured for both LPCMO films at $T \sim T_C$ in the range of photon energies, $E = 1.2$–4.1 eV. For the sample with $y = 0.7$, the spectrum represents irreversible changes of reflectivity after ZFC to $T_{MI} = 98$ K (figure 3). As shown in figure 4 MRE spectra of both films reveal three maxima at phonon energies close to 1.6 (E_1), 2.7 (E_2) and 4.0 (E_3) eV. At these energies no special features were observed in the raw spectra of the reflected intensities (see figure 5). Furthermore, the distinct maxima and minima in the MRE spectrum cannot be caused by the multi-reflection interference since the phase shift between the rays, reflected at the interfaces air/LPCMO and LPCMO/MgO, changes only by about $3\pi/2$ for the considered spectral range $E = 1.2$–4.1 eV (the LPCMO refractive index was approximated by the values for

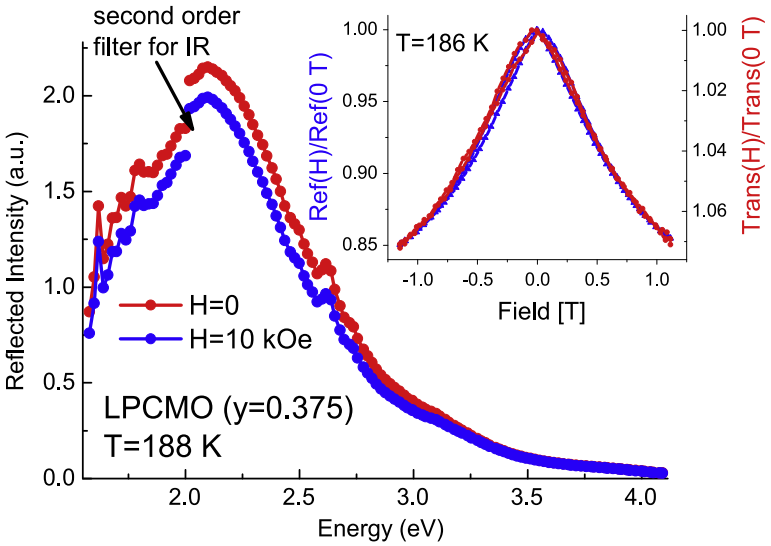

Figure 5. Raw spectra of the reflected intensity for LPCMO film ($y = 0.375$, $t = 70$ nm on MgO(100)) at $T = 188$ K with no applied field and $H = 10$ kOe. Light intensity is reduced below $E = 2.0$ eV as a high-pass filter is inserted to block the second order light from the monochromator. The inset depicts the normalized reflectance and transmittance, Trans, for the same sample at $T = 186$ K and $E = 1.5$ eV.

LSMO, taken from [25]). This could then only explain the occurrence of one broad maximum. The normalized presentations of MRE(H) curves, measured for E_1, E_2 and $E = 2.1$ eV photon energies, show the same field behavior independent on the photon energy (see the inset in figure 4). Thus, by applying a moderate magnetic field, $H = 10$ kOe, it is possible to reduce the optical reflectivity by $\sim$18% for a blue light $E_2 = 2.7$ eV ($\lambda = 460$ nm). To the best of our knowledge, such large changes of the visible light reflectance in a magnetic material were not reported until now.

4. Discussion

Before we discuss the microscopic origin of the colossal MRE some general remarks on the studied magnetooptical phenomena can be made. Firstly, the observed field-induced changes in the reflectivity are caused by *diagonal elements* of the dielectric tensor. The non-diagonal elements (linear or quadratic Kerr-effects) are not allowed [23, 24] in the used geometry with perpendicular incidence of light and magnetic field parallel to the [100] crystallographic direction of the film. Secondly, the observed MRE is a volume effect since light penetration depth [25], $t = 1/\alpha \sim 100$ nm, (α is absorption coefficient) exceeds the film thickness, $d = 70$ nm. This is also illustrated by the similar field dependences of the optical transmittance and reflectance (see inset in figure 5). Thirdly, a counterintuitive reduction of optical reflectivity for a metallic state (optical conductivity $\sigma(\omega)$ should be proportional to the dc conductivity, $\sigma(0)$, in the Drude picture [26]) is well-known for correlated metals [17, 18] undergoing a MI transition and was explained within the spectral weight transfer from the inter-band to the intra-band optical transitions.

A specific feature of LPCMO is related to the fact that MI and FM transitions develop through a phase separated state, in which FM nanodomains are AFM coupled by correlated JT polarons [7]. Close to phase transition the existence of short range spin (AFM) correlations between Mn ions may affect the inter-band optical transitions between spin polarized d-bands. The temperature- and/or field-induced appearance of long range FM order would suppress the probability of such transitions. Indeed, a reduction of optical reflectivity, $\Delta\mathrm{Ref}(T)/\mathrm{Ref}(T = 240\,\mathrm{K} > T_C)$, was observed (see figure 1(b)) by cooling the film into the FM state; the reflectivity scales apparently with $M(T)$ and most changes occur in the vicinity of T_C. Similarly, the field-induced effect (MRE) is also maximal close to T_C (see figures 2, 3) and vanishes at low temperatures ($T \ll T_C$). Thus, optical conductivity in LPCMO is not sensitive to the magnetic domain structure in a homogeneous FM metallic phase in agreement with considerations of Bennet and Stern [27] that diagonal elements of the optical conductivity tensor should be quadratic functions of the magnetization. In contrast, close to T_C the observed large hysteretic MRE and CMR (see figures 2 and 3) for relatively low magnetic fields, $H = 0$–$10\,\mathrm{kOe}$, point out the relevance of the magnetic domain structure. Moreover, the existence of two MRE minima (maxima in reflectivity) at coercive fields $H_c \approx \pm 200\,\mathrm{Oe}$ and $\pm 800\,\mathrm{Oe}$ for $y = 0.375$ and $y = 0.7$, respectively, infers that the optical conductivity is maximal in a demagnetized state with $M = 0$. Recently we have shown [7], that in LPCMO films with $y = 0.4$ an intrinsic AFM coupling, actuated by correlated polarons, stabilizes a highly insulating state close to T_C due to the antiparallel alignment of spins of adjacent magnetic nanodomains, $R \sim 6$–$8\,\mathrm{nm}$, as sketched in the inset in figure 3(b). As a result, two CMR(H_c) minima appear in close correlation with two minima in MRE(H_c). Hence, the AFM correlations between Mn^{3+} and Mn^{4+} ions are important not only for CMR but also for MRE.

The related inter-site optical transitions should involve the t_{2g} and e_g states of Mn with different oxidation states. Being mediated by (p–d) hybridization they are not forbidden by dipole selection rules as on-site transitions [28]. Actually, on-site transitions do not depend on the magnetic state, since the relative orientation of t_{2g}- and e_g-spins is fixed by strong on-site Hund's coupling. Moreover, charge transfer transitions involving the O_{2p} states should also not depend on the spin order due to their double occupancy. We suggest the following inter-site transitions are responsible for the measured MRE spectra, shown in figure 4. The peak centered around $E_1 = 1.5\,\mathrm{eV}$ is ascribed to (e_g–e_g) transitions between Mn^{3+} and Mn^{4+} ions with parallel to t_{2g} core spins [14, 20, 28, 29]. Above T_C the excitation energy is determined by $E_1 = E_B + 1/2E_{JT} \approx 1.2\,\mathrm{eV}$ (the values $E_B \sim E_{JT} = 0.8\,\mathrm{eV}$ are taken from [2]). Since the octahedron of the Mn^{4+} ion can be compressed according to a breathing mode, E_B, so that the state after the electron transfer is excited, the additional excitation energy of $E_B \approx E_{JT}$ has to be added [28, 30]. The temperature- and/or magnetic-field-induced ordering of t_{2g} spins favors delocalization of e_g electrons by reducing the number of JT distorted octahedra [19] as observed by neutron scattering [8, 9]. Thus, with an increase of spin order the spectral weight of this transition is shifted to lower frequencies. The second feature, centered around $E_2 = 2.7\,\mathrm{eV}$, is assigned to the (e_g–e_g) transition between Mn^{3+} and Mn^{4+} ions with antiparallel t_{2g} spins with excitation energy of $E_2 = E_B + 1/2E_{JT} + J_H \approx 3.2\,\mathrm{eV}$ [28, 31]. Due to the antiparallel orientation of e_g- and t_{2g} electron spins in the final state, Hund's coupling energy J_H has to be added. Finally, the maximum around 4.0 eV can be caused by (e_g–e_g) transitions between two Mn^{3+} ions with antiparallel t_{2g} spins where the excitation energy, $E_3 = E_{JT} + J_H + U \approx 4.1\,\mathrm{eV}$, is additionally increased by the Coulomb repulsion U. For a FM ordering the probability of E_2 and E_3 transitions is apparently reduced. Note that MRE in the UV-range is much smaller (see

figure 4), since for high photon energies the charge transfer transitions involving O_{2p} states, which are not sensitive to the spin order, also contribute to the absorption of photons [27, 28]. Earlier theoretical calculations [14, 15] predicted a magnetic-field-induced reduction of optical conductivity for $E > 1.0$ eV. However, the pronounced MRE spectral features were not present most probably because electronic correlations, i.e. Hund's coupling and Coulomb repulsion, were neglected.

The interpretation given above allows one to establish a clear connection between the simultaneously recorded CMR(H) and MRE(H) curves (see figures 2 and 3) in LPCMO films. The coexisting FM metallic and AFM COI polaronic phases close to a first order phase transition [7] result in a highly resistive state for $H = 0$. An applied magnetic field melts the AFM polaronic phase, favoring FM metallic domains and yielding a decrease of both resistance (MRE) and reflectivity (MRE). Besides this phase transformation the effect of magnetic field on the intrinsic electronic properties of the FM metallic phase can be neglected, since magnetic field energy is too small to compensate thermal fluctuations in the FMM phase. Indeed, a very small MRE $< 0.5\%$ was observed in LSMO films [12], which is a classical double-exchange material with second-order (continuous) phase transition and without phase separation. However, both field- and temperature-induced changes of the reflectance in LPCMO close T_C are large and comparable with each other $\sim$10–20% (see figures 1(b) and 2). This evidences a highly susceptible phase separated state (or mixed phase) close to a very sharp first-order phase transition—a low magnetic field of a few kOe is able to actuate a significant reduction of optical reflectivity.

In summary, a 'colossal MRE' with reflectivity changes up to -18% for visible light in applied field $H = 10$ kOe was observed in thin LPCMO films with Pr-doping, $y = 0.375$ and 0.7. A close similarity between the field-induced changes of the reflectivity (MRE) and of the resistance (CMR) points out their same origin, i.e. phase separation. A spectral behavior of MRE could be rationalized within the inter-site (e_g–e_g) transitions, the probability of which and, hence, optical conductivity depends on the short range ordering of t_{2g} spins of Mn^{3+} and Mn^{4+} ions.

Acknowledgment

The authors would like to thank C Ballani for the help in sample preparation, M Michelmann for useful discussions. Financial support by the Deutsche Forschungsgemeinschaft (DFG) via SFB 1073 TP B4 and EU FP7 (IFOX Project, Grant No. NMP3-LA-2010-246102) is acknowledged. This publication was supported financially by the Open Access Grant Program of the German Research Foundation (DFG) and the Open Access Publication Fund of the University of Göttingen.

References

[1] von Helmolt R *et al* 1993 *Phys. Rev. Lett.* **71** 2331
[2] Dagotto E 2003 *Nanoscale Phase Separation and Colossal Magnetoresistance* (Berlin: Springer)
[3] Uehara M, Mori S, Chen C H and Cheong S-W 1999 *Nature* **399** 560
[4] Mayr M *et al* 2001 *Phys. Rev. Lett.* **86** 135
[5] Burgy J *et al* 2001 *Phys. Rev. Lett.* **87** 277202

[6] Moreo A *et al* 2000 *Phys. Rev. Lett.* **84** 5568
[7] Moshnyaga V *et al* 2014 *Phys. Rev.* B **89** 024420
[8] Dai P *et al* 2000 *Phys. Rev. Lett.* **85** 2553
[9] Adams C P, Lynn J W, Mukovskii Y M, Arsenov A A and Shulyatev D A 2000 *Phys. Rev. Lett.* **85** 3954
[10] Kiryukhin V, Koo T Y, Ishibashi H, Hill J P and Cheong S-W 2003 *Phys. Rev.* B **67** 064421
[11] Moshnyaga V and Samwer K 2011 *Ann. Phys.* **523** 652
[12] Lee H J, Kim K H, Kim M W, Noh T W, Kim B G, Koo T Y, Cheong S-W, Wang Y J and Wei X 2002 *Phys. Rev.* B **65** 115118
[13] Jacquet J C and Valet T 1995 A new magnetooptical effect discovered on magnetic multilayers: the magnetorefractive effect *Magnetic Ultrathin Films, Multilayers and Surfaces* ed E Marinero (Pittsburgh: Materials Research Society) p 477
[14] Laad M S, Craco L and Müller-Hartmann E 2004 *New J. Phys.* **6** 157
[15] Alexandrov A S and Bratkovsky A M 1999 *Phys. Rev.* B **60** 6215
[16] Boris A V *et al* 1999 *Phys. Rev.* B **59** R697
[17] Moritomo Y *et al* 1997 *Phys. Rev.* B **56** 5088
[18] Imada M, Fujimori A and Tokura Y 1998 *Rev. Mod. Phys.* **70** 1221
[19] Millis A J, Littlewood P B and Shraiman B I 1996 *Phys. Rev. Lett.* **77** 175
[20] Hrabovsky D 2009 *Phys. Rev.* B **79** 052401
[21] Hühn S *et al* 2013 *J. Appl. Phys.* **113** 17D701
[22] Moshnyaga V *et al* 1999 *Appl. Phys. Lett.* **74** 2842
[23] Moog E R, Liu C, Bader S D and Zak J 1989 *Phys. Rev.* B **39** 6949
[24] Hamrle J *et al* 2007 *J. Phys. D: Appl. Phys.* **40** 1563
[25] Liu H L *et al* 2006 *J. Appl. Phys.* **99** 043908
[26] Ashcroft N W and Mermin N D 1976 *Solid State Physics* (Boston, MA: Cengage Learning Services)
[27] Bennett H S and Stern E A 1965 *Phys. Rev.* **137** A448
[28] Quijada M *et al* 1998 *Phys. Rev.* B **58** 16093
[29] Kaplan S G *et al* 1996 *Phys. Rev. Lett.* **77** 2081
[30] Radaelli P G, Cox D E, Marezio M and Cheong S-W 1997 *Phys. Rev.* B **55** 3015
[31] Lee H J *et al* 1999 *Phys. Rev.* B **60** 5251